THE ASTROPHYSICAL JOURNAL, **252**:156–171, 1982 January 1

AN ULTRAVIOLET STUDY OF HIGH VELOCITY INTERSTELLAR LINES IN THE CARINA NEBULA

NOLAN R. WALBORN[1]
Cerro Tololo Inter-American Observatory[2]

AND

JAMES E. HESSER[1]
Dominion Astrophysical Observatory, Herzberg Institute of Astrophysics
Received 1981 January 15; accepted 1981 June 1

ABSTRACT

With high resolution observations from the *International Ultraviolet Explorer*, an analysis has been made of interstellar absorption lines in the spectra of stars within the Carina Nebula (NGC 3372), where unusually complex, high velocity profiles were known to exist from earlier Ca II data. The high velocity structure is most pronounced in the low ionization ultraviolet lines (single ionized metals and O I). The extremely strong Mg II and C II, C II* lines reveal a number of new components with velocities even higher than those seen optically, and the total velocity range observed is 550 km s^{-1}. A curve-of-growth analysis for several of the best observed components indicates that some depletion persists, but substantially less than toward ζ Oph; and the large C II*/C II ratios indicate high densities in the high velocity material.

These velocities correspond to temperatures of a few million degrees, suggesting a relationship between the interstellar line motions and the surprising *Einstein* Observatory X-ray results in this region. Such energetic phenomena may have significant implications for the dynamics and evolution of giant H II regions.

Subject headings: interstellar: abundances — nebulae: H II regions — nebulae: individual — ultraviolet: spectra

I. INTRODUCTION

Unexpectedly complex and energetic motions were found to exist within the Carina Nebula (NGC 3372), from observations of the interstellar Ca II absorption lines in the spectra of members of the Eta Carinae association (Walborn and Hesser 1975). A total velocity range of 330 km s^{-1} was measured, including high positive as well as negative velocities, and as many as six components were seen in a single spectrum with a resolving power of 2×10^4. From the observation of simple, low velocity Ca II profiles toward association members in the outer parts of the nebula, as well as from the very small angular scale of variation among the complex profiles in the inner region, it was concluded that the high velocity material is located within the H II region, or in its very immediate foreground. It is of interest to investigate this rather unprecedented phenomenon further, by means of the far more extensive range of interstellar chemical species and ionization states accessible in the space ultraviolet wavelengths. Such an investigation has been made possible by the capabilities of the echelle spectrographs on board the *International Ultraviolet Explorer* satellite (Boggess *et al.* 1978*a*). A preliminary survey of the results has been given by Hesser and Walborn (1980).

The ultraviolet interstellar spectra show that even higher velocities than those seen optically are present in the Carina Nebula, and that the high velocity structure is strongest in the low ionization species; the latter are the principal subject of the present paper. Measurements of the high ionization and excited-state lines (other than C II*) will be presented subsequently (Hesser and Walborn 1982). Concurrently, high resolution optical observations of the Ca II and Na I interstellar lines in the Carina Nebula, obtained with the CTIO 4 m echelle spectrograph, have been analyzed (Walborn 1982). However, some results from these two related studies will be cited where pertinent to the discussion here.

II. OBSERVATIONS AND REDUCTIONS

IUE high resolution spectra of the stars with the most interesting optical interstellar profiles known at the time were obtained, in both SWP (1200–2000 Å) and LWR (2000–3000 Å) wavelength ranges, by the authors at Goddard Space Flight Center in two 16 hour shifts during 1979 September 20–23. Fortunately the particle radiation background was low, permitting long exposures, throughout this entire period. Details of these observations are given in Table 1; all of them were obtained with the small entrance aperture.

[1] Guest Observer, *International Ultraviolet Explorer* satellite.
[2] Supported by the National Science Foundation under contract AST 78-27879.

TABLE 1

PROGRAM OBSERVATIONS

Star HD/HDE	Image Number		Exposure Time (min)	Spectral Type	V	E_{B-V}
93130	SWP	6594	100	O6III(f)	8.06	0.54
	LWR	5646	75			
93160	LWR	5666	60	O6III(f)	7.81	0.49
93162	SWP	6609	240	WN6-A	8.10	0.62
	LWR	5667	90			
93204	SWP	6597	150	O5V((f))	8.42	0.42
	LWR	5669	120			
93205	SWP	6611	60	O3V	7.75	0.37
	LWR	5647	45			
93206	SWP	6612	25	O9.7Ib:(n)	6.2v	0.42
	LWR	5670	15			
303308	SWP	6596	200	O3V((f))	8.17	0.45
	LWR	5649	100			

A number of additional high resolution spectra of stars in the Carina Nebula, observed by other *IUE* investigators for other purposes, were obtained from the Goddard Data Center. Those which have been used in the present discussion are listed in Table 2, with the corresponding entrance aperture (small or large) specified for each. All SWP spectra discussed here were processed subsequently to the mid-1979 revision of the standard photometric calibration.

The standard Goddard calibration and reduction procedures (Boggess *et al.* 1978*b*) have been applied to the spectra discussed here. However, the regions of interest in the processed spectra were replotted with the Modcomp computer at the DAO, with a uniform velocity scale of 100 km s^{-1} per inch. In some cases, redundant portions of consecutive echelle orders (when the quality was comparable in both) and multiple spectra of the same star were averaged. Equivalent widths of individual interstellar line velocity components were then measured on these plots with a planimeter, following a graphical resolution of blended features. The uncertainties in the equivalent widths are nonuniform and difficult to estimate because they are dominated by different effects in different cases. For weak features a minimum uncertainty of about 20 mÅ applies, since noise excursions in the best data reach that magnitude. The major uncertainty for stronger features is often due to the resolution of blends; however, the errors should not exceed 30% in the worst cases for which measurements are given. A more objective estimate of the equivalent width accuracies may be obtained from the vertical scatter about the curves of growth discussed in § IV*a* below.

Because more accurate results are available from the optical data (Walborn and Hesser 1975; Walborn 1982), and also because the highest resolution optical echellograms show that a number of apparently single lines in the *IUE* spectra are blends, absolute radial-velocity measurements have not been undertaken in the ultraviolet spectra. Rather, the corresponding optical heliocentric velocities have been adopted for certain well defined ultraviolet components, and other components have been measured relative to the latter on the ultraviolet plots. This procedure leads to self-consistent results both among the different ultraviolet profiles and with the optical ones. The numerical velocities quoted in this paper should be regarded as component identifications, which are generally accurate to within 10 km s^{-1}.

III. RESULTS

The lines measured were those selected from inspection of the photowrites as of the highest quality, and which were not found to be blended with other interstellar features of potentially comparable intensity. These criteria are satisfied by about twenty low ionization lines, which will be discussed here, as well as by high ionization lines from C IV, Al III, and Si IV. While these latter features do show velocity structure in some spectra, generally less than 100 km s^{-1} in extent, there are few if any clear cases of velocity correspondences with the low ionization lines, in which the component structure is much more extensive. Therefore, the high ionization lines will be discussed separately (Hesser and Walborn 1982). Equivalent widths of low ionization lines in the spectra of four stars with the best observed velocity components are given in Table 3. Less extensive measures in seven additional stars of high velocity components which are seen only in the strongest lines, or for which only SWP data were available, are given in Table 4. These remark-

TABLE 2

ARCHIVAL OBSERVATIONS

Star HD/CPD	Image Number		Exposure Time (min)	Aperture	Spectral Type	V	E_{B-V}
92740	SWP	1614	11	S	WN7-A	6.40	0.28
	LWR	1549	12	S			
	LWR	2972	15	S			
93129A	SWP	2133	20	S	O3If*	7.3	0.54
	LWR	2599	25	S			
93131	SWP	1591	5	S	WN6-A	6.48	0.15
	LWR	1527	7	S			
93205	SWP	6367	50	S	O3V	7.75	0.37
	SWP	6395	50	S			
	SWP	6418	35	S			
	SWP	6436	35	S			
93222	SWP	6926	50	S	O7III((f))	8.11	0.37
93250	SWP	1618	50	S	O3V((f))	7.38	0.47
	SWP	2782	50	S			
	SWP	2783	70	S			
	LWR	2476	26	S			
93403	SWP	2625	50	S	O5III(f)v	7.28	0.53
-59°2600	SWP	7021	100	L	O6V((f))	8.61	0.53
-59°2603	SWP	7022	80	L	O7V((f))	8.77	0.46

able interstellar profiles will be discussed individually below. Finally, some comments on the interstellar spectra of four stars in which no distinct velocity components could be measured are also included.

a) *The Most Intricate Profiles*

i) *HD 93204 and HD 93205*

These two stars, separated by just 20″ or $\sim \frac{1}{4}$ pc in projection, provide a good example of the small spatial scale of variation among the interstellar profiles (Walborn and Hesser 1975). Four ultraviolet interstellar profiles in the spectrum of each are shown in Figures 1 and 2. At first glance the Mg I and Mg II profiles appear unrelated, but on closer inspection, the differences are seen to be due to noise, blending, and saturation effects on the comparison between a weak and a strong line, and the same velocity components are present in both ionization stages. The $+100$ km s^{-1} feature in HD 93205, barely detected in Ca II even on the new 4 m echelle plate, is seen to be quite strong in the ultraviolet lines. In fact, it is stronger than its counterpart in HD 93204, whereas the opposite is true in Ca II; this may be a difficulty with the assumption in the analysis below, that the feature is produced by the same "cloud" in both spectra.

The components at -20 and -40 km s^{-1} incipiently resolved in the Si II line are judged to be real because they are reproducible between the two stars, as well as among the several observations available for HD 93205. Furthermore, components near those velocities are well resolved in the optical Na I lines. This resolving power (1.5×10^4) is attained in optimum *IUE* spectra; another example will be seen below. The $+55$ km s^{-1} component in HD 93204 was not detected in the 1.5 m Ca II data, but it is present on the new 4 m plate.

ii) *HDE 303308*

Several ultraviolet interstellar profiles are shown in Figure 3. Six velocity components in Ca II were resolved by Walborn and Hesser (1975), but a non-image-tube echellogram (resolving power 6×10^4) now shows that four of them are double, and that the -100 km s^{-1} feature in the *IUE* profiles is actually a blend of (at least) four distinct components. Similarly, while the $+70$ and $+90$ km s^{-1} components are incipiently resolved in the Mg I and Fe II lines shown in Figure 3, they are completely blended in all the other ultraviolet lines. Hence further analysis of these profiles has not been included in § IV below.

iii) *CPD $-59°2600$ and CPD $-59°2603$*

Only SWP data are available for these two stars; the interstellar C II, C II* profiles in the spectra of both are shown in Figure 4. All of the ultraviolet high velocity components in CPD $-59°2600$ are well marked in Ca II on an image-tube echellogram (resolving power 3×10^4). On the contrary, in CPD $-59°$ 2603 only the -220 km

TABLE 3

EQUIVALENT WIDTHS (mÅ)

<table>
<tr><th></th><th></th><th colspan="2">HD 93130</th><th colspan="4">HD 93204</th><th colspan="2">HD 93205</th><th colspan="3">HDE 303308</th></tr>
<tr><th></th><th>Line (Å)</th><th>-190km/sec</th><th>+150km/sec</th><th>-90km/sec</th><th>+55km/sec</th><th>+100km/sec</th><th>+140km/sec</th><th>-90km/sec</th><th>+100km/sec</th><th>-100km/sec</th><th>+70km/sec</th><th>+90km/sec</th></tr>
<tr><td>CII</td><td>1334.5</td><td>218:</td><td>168:</td><td>210</td><td>b</td><td>b</td><td>163:</td><td>305:</td><td>330:</td><td>239:</td><td colspan="2">292</td></tr>
<tr><td>CII*</td><td>1335.7</td><td>275:</td><td>115</td><td>179:</td><td>196:</td><td>131:</td><td>156</td><td>230:</td><td>240</td><td>178:</td><td colspan="2">281</td></tr>
<tr><td>OI</td><td>1302.2</td><td>-</td><td>74:</td><td>168:</td><td>185:</td><td>62:</td><td>113</td><td>194:</td><td>165</td><td>149</td><td colspan="2">245</td></tr>
<tr><td>MgII</td><td>2795.5</td><td>455</td><td>310</td><td>403</td><td>b</td><td>b</td><td>246</td><td>533:</td><td>459</td><td>b</td><td colspan="2">567</td></tr>
<tr><td></td><td>2802.7</td><td>368</td><td>138</td><td>363</td><td>b</td><td>b</td><td>196</td><td>460:</td><td>376</td><td>b</td><td colspan="2">525</td></tr>
<tr><td>MgI</td><td>2852.1</td><td>151</td><td>76:</td><td>206</td><td>64</td><td>20</td><td>79</td><td>200</td><td>46</td><td>146</td><td>98</td><td>76</td></tr>
<tr><td>AlII</td><td>1670.8</td><td>-</td><td>-</td><td>172</td><td>125</td><td>39</td><td>57</td><td>218</td><td>128</td><td>181:</td><td colspan="2">229</td></tr>
<tr><td>SiII</td><td>1304.4</td><td>86:</td><td>29:</td><td>106</td><td>77:</td><td>-</td><td>88:</td><td>195</td><td>85:</td><td>105</td><td colspan="2">225:</td></tr>
<tr><td></td><td>1526.7</td><td>120</td><td>63</td><td>189</td><td>173</td><td>64</td><td>107</td><td>211</td><td>128</td><td>133</td><td colspan="2">244</td></tr>
<tr><td></td><td>1808.0</td><td>-</td><td>-</td><td>54</td><td>-</td><td>20:</td><td>30:</td><td>27</td><td>-</td><td>93</td><td colspan="2">74</td></tr>
<tr><td>SII</td><td>1250.6</td><td>-</td><td>-</td><td>20:</td><td>21</td><td>-</td><td>-</td><td>25:</td><td>-</td><td>19</td><td colspan="2">53</td></tr>
<tr><td></td><td>1253.8</td><td>32</td><td>-</td><td>16:</td><td>-</td><td>39</td><td>55</td><td>32:</td><td>-</td><td>40</td><td colspan="2">59</td></tr>
<tr><td>MnII</td><td>2576.1</td><td>57:</td><td>-</td><td>-</td><td>-</td><td>-</td><td>27:</td><td>-</td><td>-</td><td>-</td><td colspan="2">66</td></tr>
<tr><td></td><td>2593.7</td><td>-</td><td>-</td><td>-</td><td>-</td><td>-</td><td>-</td><td>19</td><td>28</td><td>38</td><td colspan="2">83</td></tr>
<tr><td>FeII</td><td>1608.5</td><td>61</td><td>83:</td><td>22:</td><td>-</td><td>-</td><td>-</td><td>77</td><td>39</td><td>98</td><td colspan="2">222</td></tr>
<tr><td></td><td>2373.7</td><td>-</td><td>-</td><td>126:</td><td>-</td><td>-</td><td>57:</td><td>144:</td><td>-</td><td>53:</td><td colspan="2">234:</td></tr>
<tr><td></td><td>2382.0</td><td>247</td><td>127</td><td>284</td><td>187:</td><td>98</td><td>205</td><td>305:</td><td>313</td><td>184</td><td colspan="2">362</td></tr>
<tr><td></td><td>2585.9</td><td>160</td><td>-</td><td>188</td><td>110</td><td>80:</td><td>127</td><td>214</td><td>146</td><td>143</td><td>181</td><td>228</td></tr>
<tr><td></td><td>2599.4</td><td>174</td><td>129</td><td>215</td><td>274:</td><td>72:</td><td>179</td><td>307</td><td>293</td><td>160</td><td colspan="2">468</td></tr>
</table>

b: Component too severely blended to measure.

TABLE 4
Equivalent Widths (mÅ)

Line (Å)	HD 92740	HD 93131	HD 93162		HD 93206	HD 93222		CPD −59°2600				CPD −59°2603		
	−200km/sec	−190km/sec	+160km/sec	+200km/sec	−290km/sec	−350km/sec	+80km/sec	−160km/sec	−90km/sec	+90km/sec	+120km/sec	−220km/sec	−160km/sec	+120km/sec
CII 1334.5	-	-	-	-	130	138	145	b	b	b	b	129	198	b
CII* 1335.7	22:	44:	37	61	-	b	128	b	b	b	260	b	b	162
OI 1302.2	-	-	-	45	-	-	69	49	245	109	106	80	69	110
MgII 2795.5	70	193	163	190	117	171	211	b	b	b	560 †	178	284	215
2802.7	-	82	154	158	41:	119	142	b	b	b	422 †	170	166	168
AlII 1670.8	-	-	-	-	-	-	-	-	202:	-	154:	28:	77	-
SiII 1304.4	-	-	18:	34	-	-	55:	42	175	22:	147:	25	50	-
1526.7	-	-	28:	65	-	-	30:	-	204	52	122	43	75	79
1808.0	-	-	-	-	-	-	-	-	57	-	-	-	-	-
FeII 1608.5	-	-	-	-	-	-	-	-	97	-	56	56	46:	56
2599.4	-	-	82:	133	-	-	94	80	324	-	380 †	107	107	80

b: Component too severely blended to measure.

†: Apparently a blend of two nearly equal components separated by ~10 km/sec.

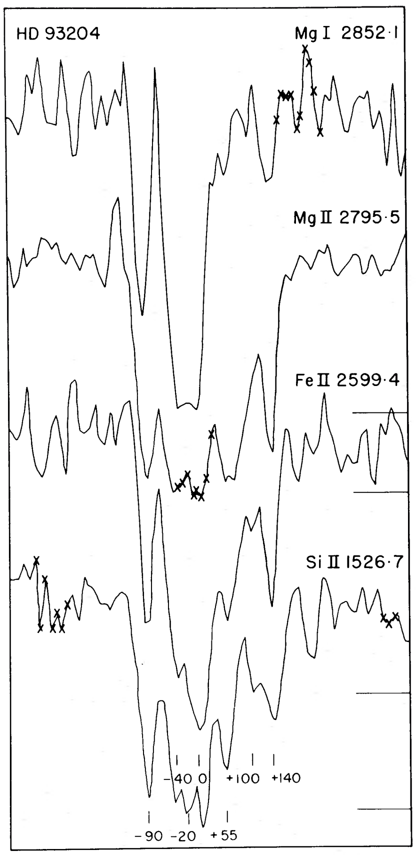

FIG. 1.

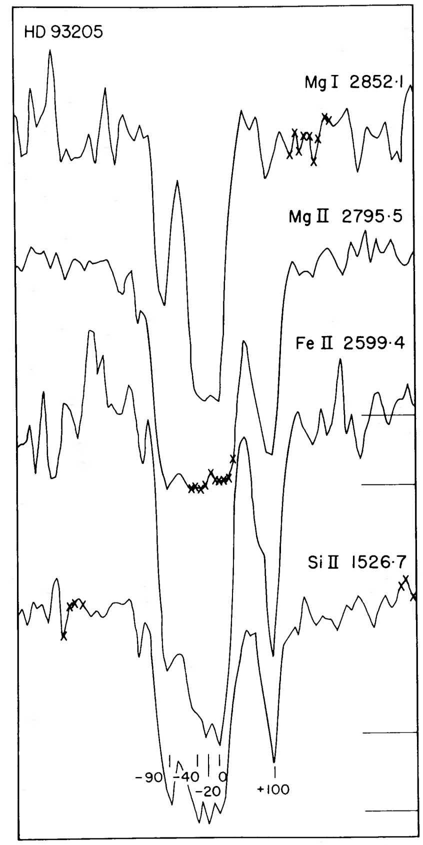

FIG. 2.

FIG. 1.—Profiles of ultraviolet interstellar absorption lines in the spectrum of HD 93204. The zero intensity level for each profile is indicated by a lateral horizontal segment, which has a length of 100 km s^{-1}. The velocities (km s^{-1}) of individual components are indicated at the bottom. The **X**'s denote the presence or proximity of a reseau mark.

FIG. 2.—Same as Fig. 1 for HD 93205

s^{-1} feature is strong in Ca II; the relatively strong -160 and $+120$ km s^{-1} ultraviolet components are not clearly detected optically. There is also some evidence in several ultraviolet lines for a component with a velocity between -70 and -90 km s^{-1} in CPD $-59°2603$. The total interstellar velocity range in this latter line of sight is 340 km s^{-1}. (See the Note added in manuscript.)

b) *New Very High Velocity Components*

i) *HD 93130*

The interstellar Ca II in this spectrum showed the highest velocity (-190 km s^{-1}) found in the Carina Nebula by Walborn and Hesser (1975), a record which has been broken several times in the *IUE* data. Moreover, the ultraviolet observations (Fig. 5) reveal a quite strong component at $+150$ km s^{-1} in this same star, which is not detected optically even on the new 4 m echelle plates, so that the interstellar velocity range is also 340 km s^{-1} in this line of sight. Several very weak Ca II and Na I absorption features at intermediate negative velocities, which evidently correspond to nearly complete absorption in the strongest ultraviolet lines, are discussed by Walborn (1982). In Ca II, there is a probable very weak component at -150 km s^{-1}, which may be blended with the -190 km s^{-1} feature in Mg II (Fig. 5).

ii) *HD 93162*

The interstellar components at 0, -30, and -60 km s^{-1}, which dominate the Ca II profiles (Walborn and Hesser 1975), are completely saturated and blended in the strong ultraviolet lines (Fig. 6). However, the latter reveal two new components at $+160$ and $+200$ km s^{-1}, which are not seen optically even on the new echellograms, and which have the largest positive velocities observed so far. Another new component at -85 km s^{-1} is seen optically, and it is well resolved in Mg I λ2852.1 with an equivalent width of 149 mÅ; hence, there is a velocity range of 285 km s^{-1} in this line of sight. There is also an interesting possible correspondence between the optical and the ultraviolet *high ionization* interstellar lines at -60 km s^{-1} in this WN-A spectrum, which will be discussed in more detail in the subsequent papers.

iii) *HD 92740 and HD 93131*

These two WN-A stars are very similar to HD 93162 in their intrinsic properties (Walborn 1973, 1974), but

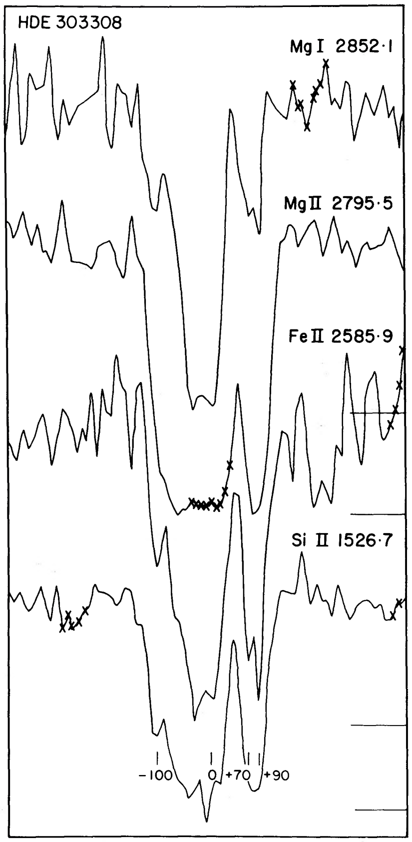

FIG. 3.—Same as Fig. 1 for HDE 303308

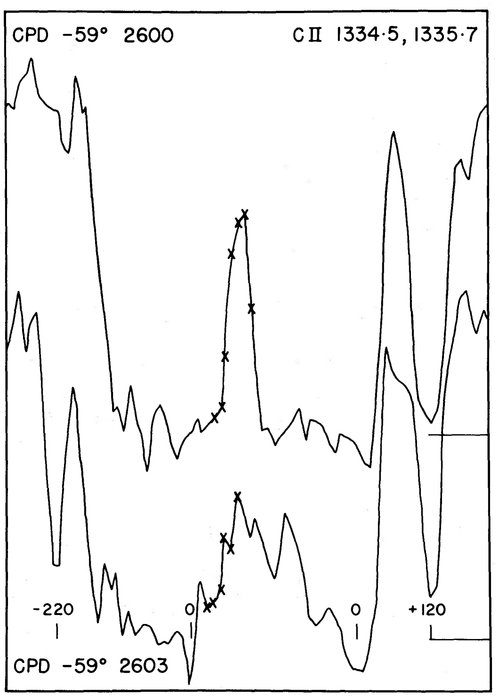

FIG. 4.—Profiles of interstellar C II λ1334.5, C II* λ1335.7 in the spectra of CPD −59°2600 (*top*) and −59°2603 (*bottom*). See the legend for Fig. 1.

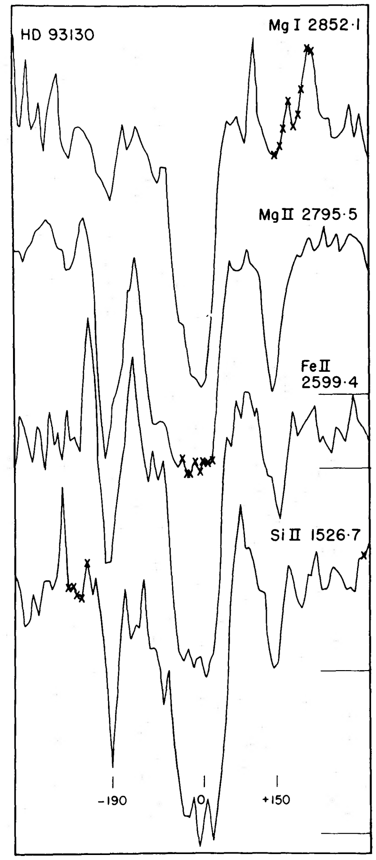

FIG. 5.—Same as Fig. 1 for HD 93130

unlike the latter they are located in the outskirts of the Carina Nebula and are over 1.5 mag brighter in *apparent* magnitude due to smaller extinction. In the 1.5 m coudé study only single, low velocity interstellar Ca II lines were found in their spectra (Walborn and Hesser 1975). However, the strong ultraviolet lines (Fig. 7) reveal strikingly similar weak components near -200 km s^{-1} in both spectra (confirmed in two LWR exposures of HD 92740); there are also stronger components at about -50 km s^{-1} in Mg II for HD 92740 and in Fe II for HD 93131, and the latter shows complete absorption in Mg II over 130 km s^{-1} FWHM.

iv) *HD 93206*

In this spectrum a weak interstellar Ca II component near -180 km s^{-1} was suspected by Walborn and Hesser (1975); it is confirmed by the new optical echellograms, but it is not clearly detected in the ultraviolet lines, possibly due to interference by a reseau mark in the case of C II λ13345. On the other hand, a stronger component at about -290 km s^{-1} is found in both Mg II and C II (Fig. 8).

v) *HD 93222*

A single, archival SWP exposure of this star, located in the southern part of the Carina Nebula, reveals the surprising interstellar C II, C II* profiles shown in Figure

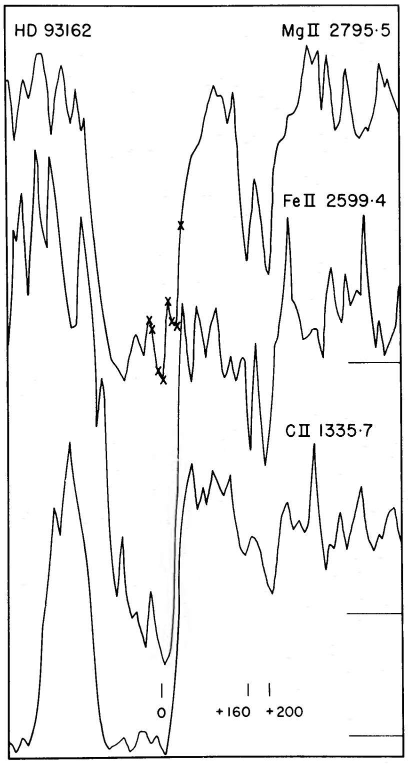

FIG. 6.—Same as Fig. 1 for HD 93162

9. Careful inspection of the photowrite gives no reason to doubt the reality of the -350 km s^{-1} feature, which has by a substantial amount the most negative velocity encountered so far in this region. (Nevertheless, it is desirable to confirm it in the Mg II lines by means of an LWR observation, and *IUE* Project Scientist's Discretionary Time has been allocated for that purpose.)

The strong $+80$ km s^{-1} component provides a good example of the large C II*/C II ratios, indicative of high densities, which are typical in these high velocity features (§ IV*c* below). The total interstellar velocity range in this line of sight is then 430 km s^{-1}. (See the Note added in manuscript.)

c) Other Stars

i) *HD 93129 A*

The available *IUE* exposures are somewhat weak in the continuum, and no distinct interstellar velocity components are detected in the low ionization lines. However, the strong Mg II and C II absorptions are at least 150 km s^{-1} FWHM. No strong high velocity features are seen optically in this spectrum.

ii) *HD 93160*

The strong interstellar Ca II profiles in this spectrum were very heavily blended in the 1.5 m coudé data (Walborn and Hesser 1975), so that component resolution with *IUE* was not expected. In addition, the *IUE* exposure is somewhat weak, apparently due to a partially successful offset attempt after the satellite guidance sensor was confused by nearby stars. Nevertheless, the very strong Mg II absorption is well defined and has 180 km s^{-1} FWHM. Several discrete velocity components are resolved in the new optical echelle data (Walborn 1982).

iii) *HD 93250*

There is good *IUE* observational coverage for this star, and there is a large range of interstellar velocities in its spectrum, but blending is very severe. The FWHM of the Mg II and C II absorptions is 240 km s^{-1}. The only discrete velocity feature in the low ionization lines is seen at about $+70$ km s^{-1} in Mg I λ2852.1, Al II λ1670.8, and Si II λ1526.7, and it corresponds to a Ca II feature measured by Walborn and Hesser (1975). However, a

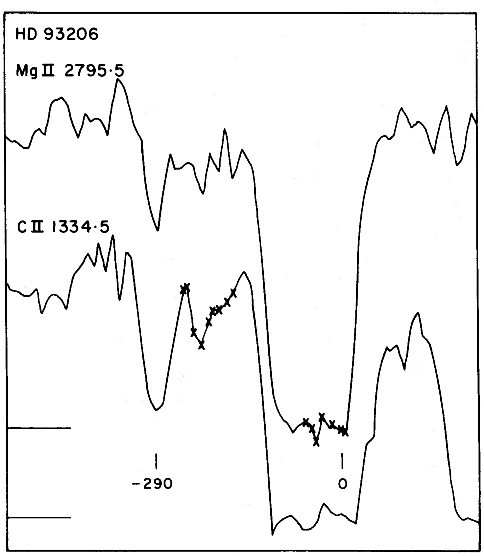

FIG. 7.—Profiles of interstellar Mg II λ2795.5 in the spectra of HD 92740 (*top*) and HD 93131 (*bottom*). See the legend for Fig. 1.

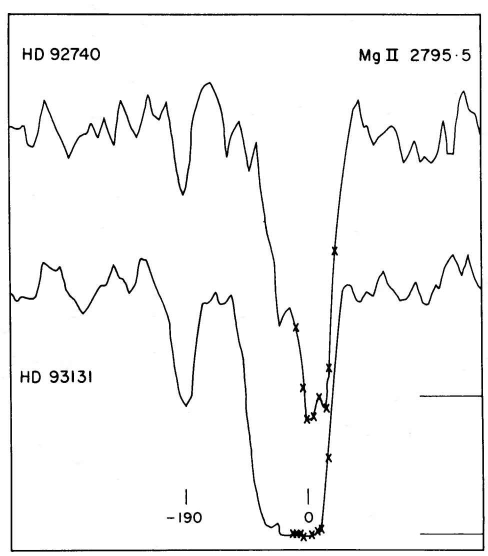

FIG. 8.—Same as Fig. 1 for HD 93206

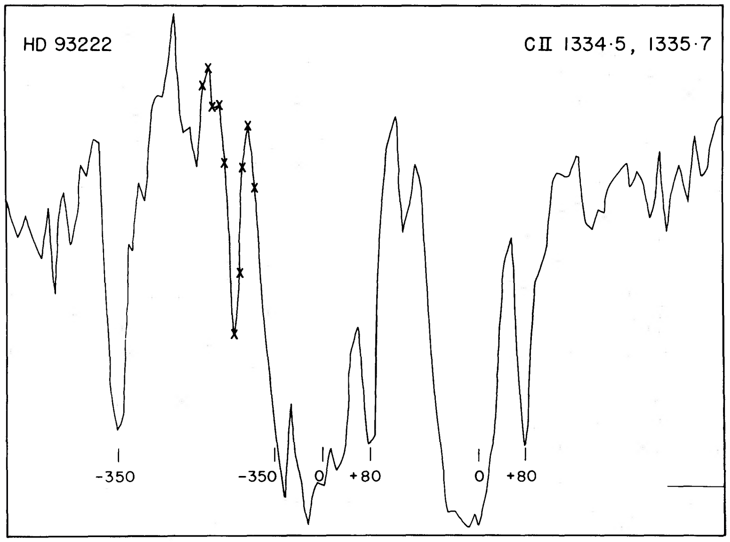

FIG. 9.—Profiles of interstellar C II λ1334.5, C II* λ1335.7 in the spectrum of HD 93222. See the legend for Fig. 1.

new non–image-tube echelle observation of Ca II shows that this feature consists of three distinct components at +50, +70, and +100 km s^{-1} (Walborn 1982), so further measurements of it in the *IUE* data have not been undertaken. The Fe II and Mn II lines are possibly double with a splitting of about 40 km s^{-1}, which again corresponds to structure in the optical. Finally, there is also very high velocity structure in the high ionization lines (Black *et al.* 1980), and the excited state O I* and O I** lines are very strong, in this spectrum (Hesser and Walborn 1982).

iv) *HD 93403*

This star is located somewhat north of the main concentrations of the association, but it appears to be at the same distance (Walborn 1973). The available *IUE* exposure is somewhat weak, and no discrete interstellar velocity components are detected. The C II absorption has roughly 130 km s^{-1} FWHM. No high velocity interstellar features are known in the optical.

IV. ANALYSIS

a) *Curves of Growth and Velocity Dispersions*

Following the methodology of Spitzer (1978), curves of growth have been constructed for the best observed interstellar velocity components not definitely known to be unresolved blends, namely those in the spectra of HD 93130, HD 93204, and HD 93205. The *f*-values were taken from Morton and Smith (1973), with the following exceptions: those for Si II λλ1526.7 (0.23) and 1808.0 (0.0055) are new determinations by Shull, Snow, and York (1981), and the value for Fe II λ1608.5 (0.0505) is from Pottasch, Wesselius, and Arnal (1980). Only the Mg II, Si II, and Fe II lines provide information about the shape of the curve, which was generally insufficient to determine it satisfactorily. Hence, the data were fitted to plots of Spitzer's theoretical curve of growth for different velocity dispersions. The best results obtained are shown in Figures 10, 11, and 12. In Figures 10 and 11, fits of the same data with two different velocity dispersions are shown in order that the uncertainties may be judged.

The dispersions of the negative velocity components in the three stars are fairly well determined to lie in the range of 10 to 15 km s^{-1}, with some preference for the larger value in the case of the −90 km s^{-1} component in HD 93204 and HD 93205 (Fig. 11). A value of 15 km s^{-1} also fits well the data for the +100 km s^{-1} component in HD 93205 (Fig. 12). On the other hand, if appears possible that a substantially smaller dispersion may be appropriate for other high positive velocity components. For instance, in Figure 12 it has been assumed that the +100 km s^{-1} component in HD 93204 is produced by the same "cloud" seen at that velocity in HD 93205, although a morphological difficulty with that assumption was noted in § III*a*(i) above. Moreover, the Fe II λ2585.9 point for HD 93204 in Figure 12 lies to the left of the curve, and the Si II λ1808.0, not shown, lies off scale to the left. The five Si II and Fe II points available in this case could be fitted by a curve with $b < 5$ km s^{-1}, although the discrepancy from the $b = 15$ km s^{-1} curve depends on only two points, both of which are denoted as uncertain measures in Table 3. Similar remarks can be made about the +140 km s^{-1} component in HD 93204, for which Fe II indicates $b \sim 10$ km s^{-1}, but Si II is better fitted with $b \sim 6$ km s^{-1}, with the discordance due primarily to one (uncertain) point in each case. Clearly, more extensive observations with higher resolution and signal to noise are required in order to answer these questions conclusively.

Fifteen km s^{-1} is just below the resolution of the *IUE* data, and one might ask whether a velocity dispersion of this magnitude indicates unresolved velocity substructure in the analyzed components. In § III, some morphological evidence in that direction was noted for the +100

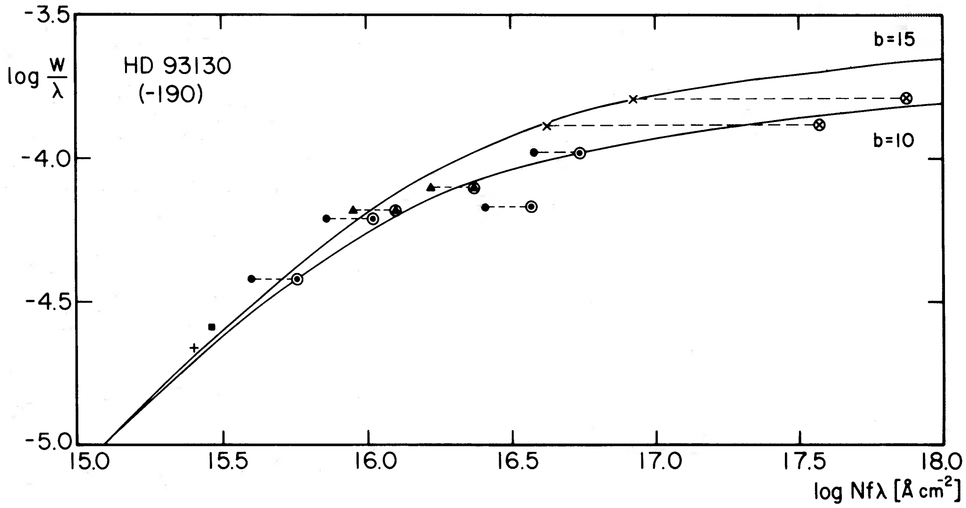

FIG. 10.—Curves of growth for the $-190 \mathrm{~km~s^{-1}}$ component in the spectrum of HD 93130. The solid lines are theoretical curves from Spitzer (1978), for $b = 15 \mathrm{~km~s^{-1}}$ (*upper*) and $b = 10 \mathrm{~km~s^{-1}}$ (*lower*). The key to the observational points is as follows: **X**'s, Mg II; *filled circles*, Fe II; *triangles*, Si II; *squares*, S II; and *crosses*, Mn II. Uncircled symbols refer to the 15 km s^{-1} curve, and circled symbols to the 10 km s^{-1} curve, except for S II and Mn II, for which the column densities were calculated from the linear relation. The same data points for the two b's are joined by horizontal dashed lines.

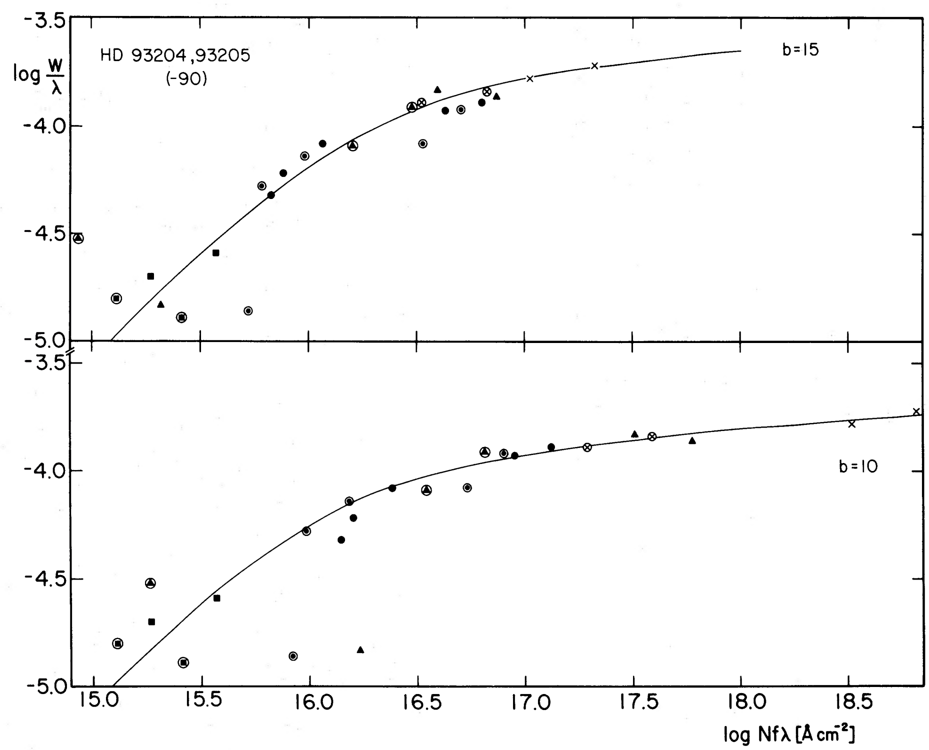

FIG. 11.—Curves of growth for the $-90 \mathrm{~km~s^{-1}}$ components in HD 93204 and 93205. *Top*, $b = 15 \mathrm{~km~s^{-1}}$; *bottom*, $b = 10 \mathrm{~km~s^{-1}}$. Theoretical curves and observational symbols are as in Fig. 10, except that here circled symbols refer to HD 93204 and uncircled symbols to HD 93205.

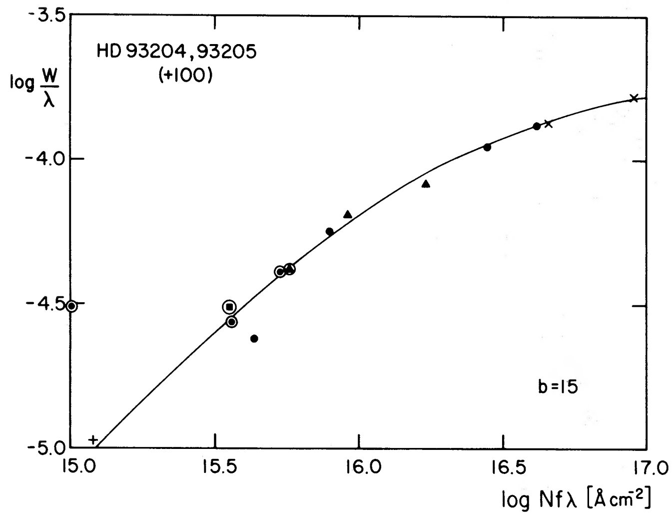

FIG. 12.—Curve of growth for the +100 km s^{-1} components in HD 93204 and 93205, for b = 15 km s^{-1}. The theoretical curve and observational symbols are as in Fig. 10, except that circled symbols refer to HD 93204 and uncircled symbols to HD 93205.

km s^{-1} feature in HD 93205 and the −190 km s^{-1} in HD 93130, and the optical echellograms definitely establish substructure in apparently discrete ultraviolet features for HDE 303308 and HD 93250. To investigate this question, velocity dispersions for several components analyzed in the ultraviolet have been measured directly from intensity tracings of the optical image-tube echellograms (resolving power 3 to 4 × 10^4); they are given in Table 5, where b is the FWHM divided by $2(\ln 2)^{1/2}$. The results are essentially at the resolution limit of the optical plates, and they are marginally but systematically smaller than those from the ultraviolet analysis, indicating that substructure may indeed be present in some of the high velocity components of the (relatively stronger) ultraviolet lines.

b) *Column Densities, Abundances, and Depletions*

Column densities for the observed species were derived from the curves of growth and are given in Table 6. The values for S II and Mn II were calculated from the linear relation except in the case of the +140 km s^{-1} S II feature

TABLE 5

OPTICAL VELOCITY DISPERSIONS

Star	Component (km s^{-1})	Species (Ca II or Na I)	b (km s^{-1})
HD 93130	−190	K	9
		D2	8
HD 93204	−90	K	13
		D2	6
	+100	K	7
	+140	K	6
HD 93205	−90	K	10
		D2	8

in HD 93204. Results are given for two different velocity dispersions in several cases, to establish upper limits to the uncertainties in the column densities. The well known fact is illustrated that the uncertainties are not very great for the weaker lines but can reach two orders of magnitude for strongly saturated lines on the flat part of the curve of growth.

The column densities have been scaled to relative abundances by means of the assumptions that (1) the observed ionization states are the dominant ones (justified by the relative weakness or absence of high-velocity components in C I, Mg I, and Al III) and (2) that S is undepleted and has the solar abundance relative to H (e.g., Jenkins, Silk, and Wallerstein 1976). The results are also given in Table 6; the solar abundances there, as well as the depletions toward ζ Oph, are from the updated compilation by Snow (1980).

The corresponding depletions derived for the high velocity gas in the Carina Nebula are given in the final part of Table 6. Ignoring for the moment the C and O results, it appears quite generally that some depletion persists in this material, although substantially less than is observed toward ζ Oph. The apparently excessive depletions derived for O may indicate the presence of a significant amount of O II, or, alternatively, that the curves of growth are not entirely applicable to O I, a possibility if the analyzed velocity components are actually blends due to more than one "cloud" with different physical conditions (de Boer 1981). The excess C abundances resulting with the lower velocity dispersions may be taken to mean either that those dispersions are not appropriate, or that additional, weaker velocity components are contributing to the very sensitive C II lines.

The existence of depletions in this very high velocity material is somewhat surprising, since high velocity interstellar gas is usually found to be undepleted, even at velocities substantially smaller than those observed here

1982ApJ...252..156W

TABLE 6

COLUMN DENSITIES, ABUNDANCES, AND DEPLETIONS[a]

Species	Star: / Component: b:	HD 93130 −190km/sec 15km/sec	HD 93130 −190km/sec 10km/sec	HD 93130 +150km/sec ~12km/sec	HD 93204 −90km/sec 15km/sec	HD 93204 −90km/sec 10km/sec	HD 93204 +55km/sec ~12km/sec	HD 93204 +100km/sec 15km/sec	HD 93204 +140km/sec 10km/sec	HD 93204 +140km/sec ~6km/sec	HD 93205 −90km/sec 15km/sec	HD 93205 −90km/sec 10km/sec	HD 93205 +100km/sec 15km/sec
Log Column Densities (cm^{-2})													
CII		14.75	16.02	14.57	14.70	15.86	-	-	14.92	17.23	15.95	>17.6	16.33
CII*		15.43	17.45	14.08	14.44	15.21	14.95	14.10	14.80	16.90	14.91	16.38	14.97
OI		-	-	14.16	14.78	15.45	15.22	14.03	14.63	16.00	14.98	15.94	14.76
MgII		13.70	14.66	13.09	13.60	14.37	-	-	13.24	14.23	14.10	15.60	13.74
MgI		12.15	12.75	11.81	12.35	12.49	11.73	11.16	11.85	11.92	12.33	12.47	11.57
AlII		-	-	-	12.85	13.18	12.66	11.97	12.20	12.30	13.11	13.82	12.60
SiII		13.67	13.82	13.20	13.92	14.27	13.82	13.21	13.79	14.35	14.31	15.23	13.68
SII		14.33	14.33	-	14.28	14.28	14.45	14.42	14.72	14.87	14.44	14.44	-
MnII		12.53	12.53	-	-	-	-	-	12.20	12.20	12.16	12.16	12.32
FeII		13.69	13.85	13.12	13.81	14.01	13.54	12.84	13.52	14.46	13.91	14.23	13.73
Log Abundances	Sun												
H	12.00	12.00	12.00	-	12.00	12.00	12.00	12.00	12.00	12.00	12.00	12.00	-
C	8.57	8.39	10.35	-	7.82	8.88	-	-	7.66	9.74	8.76	>10.4	-
O	8.83	-	-	-	7.71	8.38	7.98	6.82	7.12	8.34	7.75	8.71	-
Mg	7.54	6.58	7.54	-	6.53	7.30	-	-	5.73	6.57	6.87	8.37	-
Al	6.40	-	-	-	5.78	6.11	5.42	4.76	4.69	4.64	5.88	6.59	-
Si	7.55	6.55	6.70	-	6.85	7.20	6.58	6.00	6.28	6.69	7.08	8.00	-
S	7.21	7.21	7.21	-	7.21	7.21	7.21	7.21	7.21	7.21	7.21	7.21	-
Mn	5.42	5.41	5.41	-	-	-	-	-	4.69	4.54	4.93	4.93	-
Fe	7.40	6.57	6.73	-	6.74	6.94	6.30	5.63	6.01	6.80	6.68	7.00	-
Log Depletions	ζ Oph												
C	−0.56/−0.89	−0.18	+1.78	-	−0.75	+0.31	-	-	−0.91	+1.17	+0.19	>+1.83	-
O	−0.13	-	-	-	−1.12	−0.45	−0.85	−2.01	−1.71	−0.49	−1.08	−0.12	-
Mg	−1.37	−0.96	0.00	-	−1.01	−0.24	-	-	−1.81	−0.97	−0.67	+0.83	-
Al	−3.14/−3.46	-	-	-	−0.62	−0.29	−0.98	−1.64	−1.71	−1.76	−0.52	+0.19	-
Si	−1.72/−1.92	−1.00	−0.85	-	−0.70	−0.35	−0.97	−1.55	−1.27	−0.86	−0.47	+0.45	-
S	−0.12/−0.50	0	0	-	0	0	0	0	0	0	0	0	-
Mn	−1.39	−0.01	−0.01	-	-	-	-	-	−0.73	−0.88	−0.49	−0.49	-
Fe	−2.20	−0.83	−0.67	-	−0.66	−0.46	−1.10	−1.77	−1.39	−0.60	−0.72	−0.40	-

[a] For oxygen, these formally derived values are subject to the possible limitations discussed in § IV*b* of the text.

(Spitzer 1976; Jenkins, Silk, and Wallerstein 1976; McCray and Snow 1979; Cowie, Songaila, and York 1979). On the other hand, examples of high velocity gas with some residual depletion have recently been described (Pottasch, Wesselius, and Arnal 1980; Phillips, Gondhalekar, and Blades 1981). On the basis of current understanding of interstellar depletion, these results imply the presence of grains in the Carina Nebula high velocity material, a circumstance perhaps related to the high densities indicated by the C II*/C II ratios, discussed next.

c) *Electron Densities*

The ratio of the excited state line C II* λ1335.7 (actually, two lines differing in wavelength by 0.05 Å and in strength by a factor of 9) to the zero volt line C II λ1334.5, provides information about the electron densities. The convenient graphs presented by Smeding and Pottasch (1979) have been used to derive the values given in Table 7. Actually, these values may be *upper limits* in the case of high neutral densities, but the total density would then be high in any event. Unfortunately, the C II column densities derived here are the most uncertain of all, and an unphysically large ratio results for the -190 km s^{-1} feature in HD 93130. A straight mean of all the numerical entries in Table 7 yields $\langle \log N(\mathrm{C\,II^*})/N(\mathrm{C\,II}) \rangle = -0.34 \pm 0.30$, and one could adopt the view that the correct value is zero within the accuracy of the determinations. In that case, a temperature of 100 K is ruled out, and the resulting log n_e's are 1.5 for a temperature of 1000 K, and 2.0 for 10,000 K.

V. DISCUSSION

All of the stars observed here are members of the Eta Carinae association, at a distance of 2800 pc if $R = 3$ (Walborn 1973, and unpublished). Their distribution on the sky was shown by Walborn (1973) and Walborn and Hesser (1975), and most of them are seen in the interference filter photographs published by Walborn (1975). The discovery of some high velocity structure in the ultraviolet interstellar lines of the peripheral WN-A stars HD 92740 and HD 93131 does not weaken significantly the conclusion from the 1.5 m coudé study about the local nature of the high velocity material, since the very small angular scale of variation among the complex profiles still requires that they be formed very close to the stars. This latter characteristic is confirmed and extended by the new optical echelle data.

The total interstellar velocity range observed in this region stands at 550 km s^{-1}, with the positive and negative extremes seen toward HD 93162 and HD 93222, respectively. If the high velocity material consists of small clouds or filaments in chaotic motion, collisions at this full relative velocity may be occurring, and the corresponding temperature $T = 2 \times 10^6\,(v/300\ \mathrm{km\ s^{-1}})^2$ (Wallerstein and Silk 1971) will be 6.7×10^6 K, or 0.6 keV. Even if one assumes more ordered high velocity motions and collisions only with low velocity material, the temperature will still exceed 10^6 K. These energies suggest a relationship between the interstellar lines and the unexpected X-ray properties of this region discovered by the *Einstein* Observatory: not only are most of the stars observed here found to be discrete sources of X-rays, but also diffuse soft X-ray emission permeates the entire field of the Carina Nebula (Seward *et al.* 1979; Seward, private communication). Furthermore, there are evident morphological coincidences between the diffuse X-ray contours and the distributions of the stars and interstellar material. Enhancements of the X-ray emission are seen adjacent to HD 93130 and HD 93222, which have interstellar velocity ranges of 340 and 430 km s^{-1}, respectively, in their spectra. A ridge of enhanced emission approximately coincides with a "chain" of O stars just southeast of η Car, several of which show very high velocity interstellar features (Walborn 1982). It is also noteworthy that the two outer, less obscured WN-A stars HD 92740 and HD 93131 are far weaker X-ray sources (if indeed they are sources at all) than the intrinsically similar but heavily obscured HD 93162, whereas the opposite might be expected if the X-rays were due to the stellar winds alone; rather, this situation suggests that an *interaction* between the stellar wind and dense surrounding material may be responsible for the high energy phenomena. One is reminded of the "interstellar bullets" of Norman and Silk (1979). The energetics of the stellar wind hypothesis for the origin of the high velocity material is pursued further by Walborn (1982), since the new optical data extend to a number of fainter association members and hence pro-

TABLE 7
ELECTRON DENSITIES (cm^{-3})

Star	Component (km s^{-1})	b (km s^{-1})	$\log \frac{N(\mathrm{C\,II^*})}{N(\mathrm{C\,II})}$	log n_e for T = 100 K	1000 K	10,000 K
HD 93130	−190	15	+0.68	...	...	...
		10	+1.43	...	...	...
	+150	~12	−0.49	+0.7	+0.7	1.1
HD 93204	− 90	15	−0.26	+1.2	+1.0	1.4
		10	−0.65	+0.5	+0.5	0.9
	+140	10	−0.12	+2.0	+1.2	1.7
HD 93205	− 90	15	−1.04	+0.1	+0.1	0.6
		10	< −1.22	< −0.2	< −0.1	<0.4
	+100	15	−1.36	−0.3	−0.2	0.3

vide better constraints on the spatial extent of a given high velocity component.

One further apparent spatial relationship is worth noting. The near-ultraviolet photograph published by Seward *et al.* (1979) shows that at those wavelengths the brightest spot in the southern part of the Carina Nebula coincides with an X-ray contour, just west of HD 93222; moreover, this spot is not centered on any of the bright O stars. Further investigation of this part of the nebula is indicated, to determine whether this ultraviolet emission might be collisionally induced, as developed by Raymond (1979) and Shull and McKee (1979).

An alternative explanation for the high-energy phenomena in the Carina Nebula region could be an old supernova remnant, as discussed by Seward *et al.* (1979). The only other region in the Galaxy known to have such extreme interstellar line velocity structure is that of the Vela SNR (Wallerstein and Silk 1971; Jenkins, Silk, and Wallerstein 1976), although there is higher ionization and essentially no depletion in that case. Less extreme high velocity interstellar features, but of low ionization as in the Carina Nebula, are seen toward the Orion association (Cowie, Songaila, and York 1979) and the SNR Shajn 147 (Phillips, Gondhalekar, and Blades 1981), with residual depletions also observed in the latter case. Very high velocity, low ionization interstellar lines have also been found toward the SNR IC 443 by Gondhalekar and Phillips (1980). If a supernova is the cause of the high energy phenomena in the Carina Nebula, however, then the various apparent relationships noted above between the diffuse X-ray emission and the presently observed stars would have to be fortuitous.

An additional source of high energies within the Carina Nebula is η Car itself. Very high velocities are found in its compact, expanding nebulosity, evidently ejected during the past few centuries (Walborn, Blanco, and Thackeray 1978). If η Car has produced such outbursts for thousands of years, it could conceivably have affected a larger extent of the surrounding H II region (Walborn and Liller 1977; Allen 1979).

Whichever the specific origin of the high interstellar velocities and X-ray emission observed in the Carina Nebula, these energetic phenomena are likely to be evidence of the mechanisms whereby a rich association of massive young stars dissipates the remnants of the gas and dust from which it formed.

N. R. W. wishes to thank Sidney van den Bergh, Jim Hesser, and the DAO staff for their pleasant hospitality in Victoria while this work was in progress. He also thanks Victor Blanco/CTIO and Michael Penston/European Space Agency for travel support to attend the 1980 October ESA Interstellar Line Workshop at Villafranca del Castillo (*Nature*, **289**, 123 [1981]), where discussions with colleagues contributed to the presentation of these results. Helpful comments were also made by John Black and Don York. The *IUE* data plotting program at the DAO was originally written by John Hutchings and was elaborated for this work with assistance by John van Heteren. We also thank Peter Conti, Sara Heap, John Hutchings, and Yoji Kondo for authorizing early release of their *IUE* observations to us, and Wayne Warren for expediting an archival data shipment.

Note added in manuscript, in collaboration with Dr. Robert J. Panek, Computer Sciences Corporation, Goddard Space Flight Center.—The additional observations listed in Table 8 were obtained by R. J. P. on *IUE* Project Scientist's Discretionary Time 1981 January 24 and 29. All are high resolution spectra taken with the large entrance aperture. Equivalent width measurements of interstellar Mg II $\lambda\lambda$2795.5, 2802.7 and Fe II λ2599.4 in the spectra of HD 93222 and CPD −59°2600 and −59°2603 have been entered in Table 4. The following additional velocity components have been measured: in CPD −59°2600, Mg I λ2852.1 at −90 km s^{-1} (156 mÅ) and +120 km s^{-1} (106 mÅ); in CPD −59°2603, Fe II λ2599.4 at −90 km s^{-1} (207 mÅ); and in HD 93146, C II λ1334.5 at −220 km s^{-1} (158 mÅ) and C II* λ1335.7 at +60 km s^{-1} (252 mÅ). The Mg II profiles in HD 93222 and CPD −59°2603, and the C II, C II* in HD 93146, are shown in Figures 13, 14, and 15, respectively. The remarkable Mg II profiles in HD 93222 clearly confirm the interpretation of the C II, C II* (Fig. 9) discussed above. HD 93146 is located in the southern part of the Carina Nebula, close to HD 93222 and the ultraviolet-bright patch of nebulosity pointed out in the discussion above. The interstellar spectra of both stars show very high negative velocity components and more moderate high positive velocity ones, but the actual velocities toward the two stars are quite different. (The distribution on the sky of all known ultraviolet and optical interstellar velocity components in the Carina Nebula is illustrated by Walborn 1982.)

We are grateful to Dr. Albert Boggess, *IUE* Project Scientist, for the opportunity to obtain these followup observations.

TABLE 8

DISCRETIONARY OBSERVATIONS

Star HD/CPD	Image Number	Exposure Time (min)	Spectral Type	V	E_{B-V}
93146	SWP 11136	60	O6.5 V ((f))	8.44	0.34
	LWR 9804	45			
93222	LWR 9765	30	O7 III ((f))	8.11	0.37
−59°2600	LWR 9766	90	O6 V ((f))	8.61	0.53
−59°2603	LWR 9767	90	O7 V ((f))	8.77	0.46

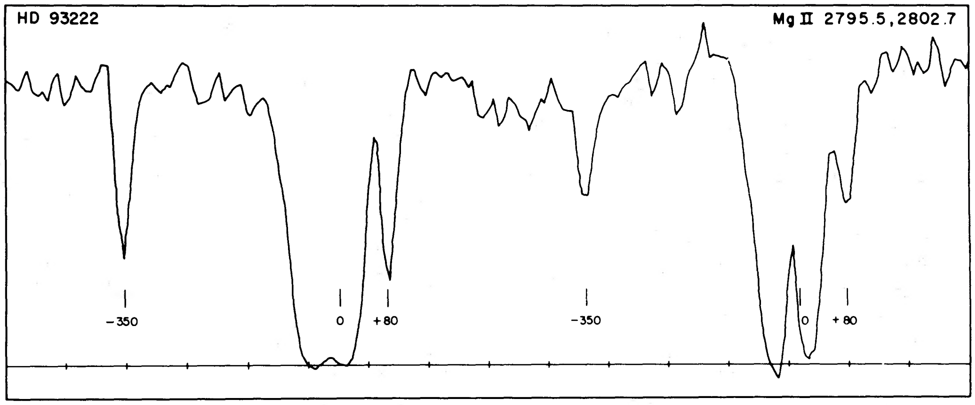

FIG. 13.—Profiles of interstellar Mg II $\lambda\lambda$2795.5, 2802.7 in the spectrum of HD 93222. Zero intensity is indicated by the horizontal line with vertical marks; the latter denote 100 km s^{-1} intervals. The heliocentric velocities (km s^{-1}) of individual components are also indicated. Compare with Fig. 9.

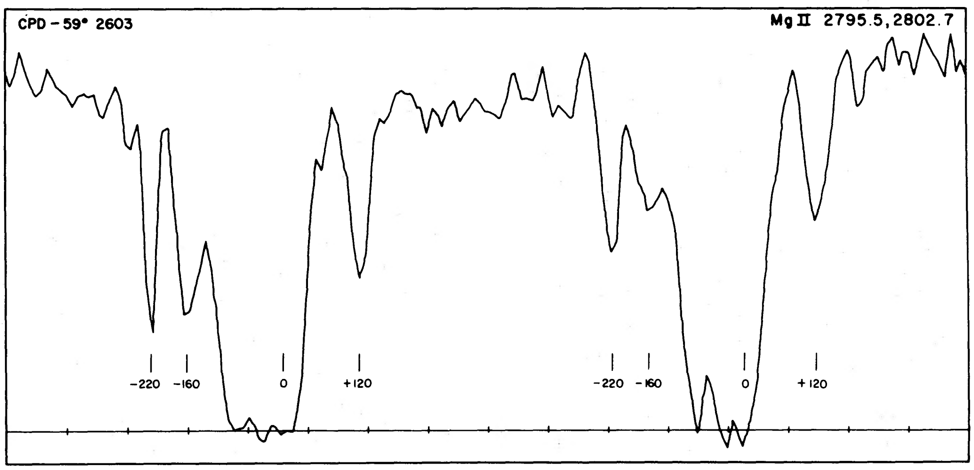

FIG. 14.—Same as Fig. 13 for CPD −59°2603. See also Fig. 4

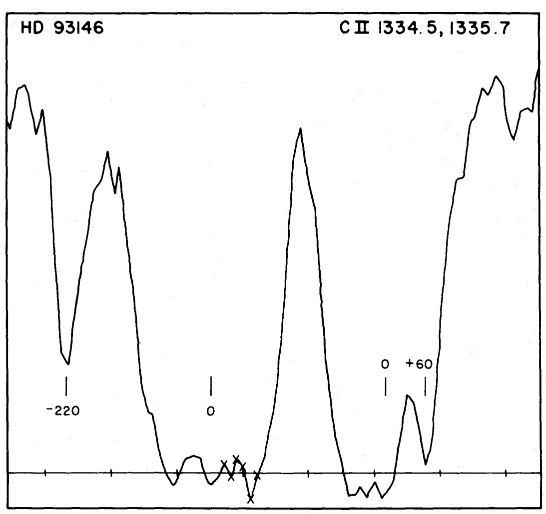

FIG. 15.—Profiles of interstellar C II λ1334.5, C II* λ1335.7 in the spectrum of HD 93146. See the legend for Fig. 13. The **X**'s denote the proximity of a reseau mark.

REFERENCES

Allen, D. A. 1979, *M.N.R.A.S.*, **189**, 1P.
Black, J. H., Dupree, A. K., Hartmann, L. W., and Raymond, J. C. 1980, *Ap. J.*, **239**, 502.
Boggess, A. *et al.* 1978*a*, *Nature*, **275**, 372.
———. 1978*b*, *Nature*, **275**, 377.
Cowie, L. L., Songaila, A., and York, D. G. 1979, *Ap. J.*, **230**, 469.
de Boer, K. S. 1981, *Ap. J.*, **244**, 848.
Gondhalekar, P. M., and Phillips, A. P. 1980, in *Second European IUE Conference* (ESA SP-157), p. 109.
Hesser, J. E., and Walborn, N. R. 1980, in *The Universe at Ultraviolet Wavelengths: The First Two Years of IUE*, ed. R. D. Chapman (NASA CP-2171), p. 571.
———. 1982. in preparation.
Jenkins, E. B., Silk, J., and Wallerstein, G. 1976, *Ap. J.* (*Letters*), **209**, L87 and *Ap. J. Suppl.*, **32**, 681.
McCray, R., and Snow, T. P., Jr. 1979, *Ann. Rev. Astr. Ap.*, **17**, 213.
Morton, D. C., and Smith, Wm. H. 1973, *Ap. J. Suppl.*, **26**, 333.
Norman, C., and Silk, J. 1979, *Ap. J.*, **228**, 197.
Phillips, A. P., Gondhalekar, P. M., and Blades, J. C. 1981, *M.N.R.A.S.*, **195**, 485.
Pottasch, S. R., Wesselius, P. R., and Arnal, E. M. 1980, in *Second European IUE Conference* (ESA SP-157), p. 13.
Raymond, J. C. 1979, *Ap. J. Suppl.*, **39**, 1.
Seward, F. D., Forman, W. R., Giacconi, R., Griffiths, R. E., Harnden, F. R., Jr., Jones, C., and Pye, J. P. 1979, *Ap. J.* (*Letters*), **234**, L55.
Shull, J. M., and McKee, C. F. 1979, *Ap. J.*, **227**, 131.
Shull, J. M., Snow, T. P., and York, D. G. 1981, *Ap. J.*, **246**, 549.
Smeding, A. G., and Pottasch, S. R. 1979, *Astr. Ap. Suppl.*, **35**, 257.
Snow, T. P. 1980, at ESA Workshop on Interstellar Absorption Lines, Villafranca del Castillo.
Spitzer, L. 1976, *Comments on Ap.*, **6**, 177.
———. 1978, *Physical Processes in the Interstellar Medium* (New York: J. Wiley and Sons).
Walborn, N. R. 1973, *Ap. J.*, **179**, 517.
———. 1974, *Ap. J.*, **189**, 269.
———. 1975, *Ap. J.* (*Letters*), **202**, L129.
———. 1982. *Ap. J. Suppl.*, **48**, in press.
Walborn, N. R., Blanco, B. M., and Thackeray, A. D. 1978, *Ap. J.*, **219**, 498.
Walborn, N. R., and Hesser, J. E. 1975, *Ap. J.*, **199**, 535.
Walborn, N. R., and Liller, M. H. 1977, *Ap. J.*, **211**, 181.
Wallerstein, G., and Silk, J. 1971, *Ap. J.*, **170**, 289.

James E. Hesser: Dominion Astrophysical Observatory, 5071 West Saanich Road, Victoria, B.C. V8X 4M6, Canada

Nolan R. Walborn: Cerro Tololo Inter-American Observatory, Casilla 603, La Serena, Chile